Article

Cell Reports

Satb1 Overexpression Drives Tumor-Promoting Activities in Cancer-Associated Dendritic Cells

Graphical Abstract

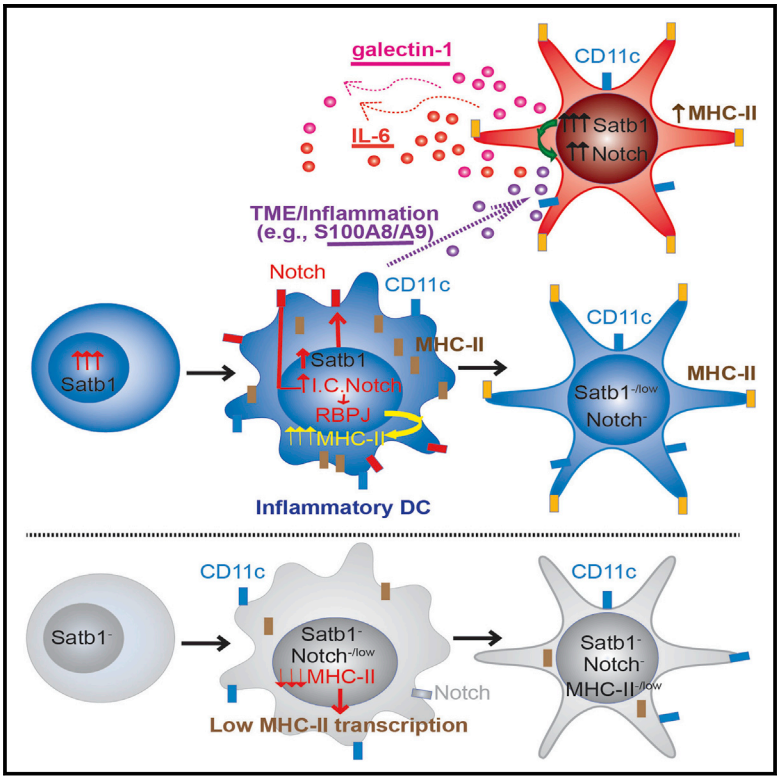

Highlights

- Mature inflammatory dendritic cells (DCs) infiltrate solid ovarian cancers
- Satb1 regulates the differentiation of conventional $CD4^+$ DCs
- Satb1 regulates Notch signaling, which turns on MHC II in inflammatory DCs
- Unremitting expression of Satb1 drives immunosuppressive DCs

Authors

Amelia J. Tesone, Melanie R. Rutkowski, Eva Brencicova, ..., Gabriel A. Rabinovich, Andrew V. Kossenkov, Jose R. Conejo-Garcia

Correspondence

jrconejo@wistar.org

In Brief

Tesone et al. report that dynamic expression of Satb1 regulates the generation and immunostimulatory activity of conventional dendritic cells (DCs) and the acquisition of MHC II expression in inflammatory DCs. However, relentless Satb1 overexpression in tumor-associated DCs converts them into tolerogenic/pro-inflammatory cells that contribute to malignant progression.

Accession Numbers

GSE76776

Tesone et al., 2016, Cell Reports *14*, 1774–1786
February 23, 2016 ©2016 The Authors
http://dx.doi.org/10.1016/j.celrep.2016.01.056

OPEN ACCESS
CellPress

Cell Reports
Article

Satb1 Overexpression Drives Tumor-Promoting Activities in Cancer-Associated Dendritic Cells

Amelia J. Tesone,[1] Melanie R. Rutkowski,[1] Eva Brencicova,[1] Nikolaos Svoronos,[1] Alfredo Perales-Puchalt,[1] Tom L. Stephen,[1] Michael J. Allegrezza,[1] Kyle K. Payne,[1] Jenny M. Nguyen,[1] Jayamanna Wickramasinghe,[2] Julia Tchou,[3] Mark E. Borowsky,[4] Gabriel A. Rabinovich,[5] Andrew V. Kossenkov,[2] and Jose R. Conejo-Garcia[1,*]
[1]Tumor Microenvironment and Metastasis Program, the Wistar Institute, Philadelphia, PA 19104, USA
[2]Center for Systems and Computational Biology, the Wistar Institute, Philadelphia, PA 19104, USA
[3]Division of Endocrine and Oncologic Surgery, Department of Surgery, University of Pennsylvania, Philadelphia, PA 19104-1693, USA
[4]Helen F. Graham Cancer Center, Christiana Care Health System, 4701 Ogletown-Stanton Road, Newark, DE 19713, USA
[5]Laboratorio de Inmunopatología, Instituto de Biología y Medicina Experimental (IBYME-CONICET), C1428ADN Buenos Aires, Argentina
*Correspondence: jrconejo@wistar.org
http://dx.doi.org/10.1016/j.celrep.2016.01.056

SUMMARY

Special AT-rich sequence-binding protein 1 (Satb1) governs genome-wide transcriptional programs. Using a conditional knockout mouse, we find that Satb1 is required for normal differentiation of conventional dendritic cells (DCs). Furthermore, Satb1 governs the differentiation of inflammatory DCs by regulating major histocompatibility complex class II (MHC II) expression through Notch1 signaling. Mechanistically, Satb1 binds to the Notch1 promoter, activating Notch expression and driving RBPJ occupancy of the *H2-Ab1* promoter, which activates MHC II transcription. However, tumor-driven, unremitting expression of Satb1 in activated *Zbtb46*$^{+}$ inflammatory DCs that infiltrate ovarian tumors results in an immunosuppressive phenotype characterized by increased secretion of tumor-promoting Galectin-1 and IL-6. In vivo silencing of *Satb1* in tumor-associated DCs reverses their tumorigenic activity and boosts protective immunity. Therefore, dynamic fluctuations in Satb1 expression govern the generation and immunostimulatory activity of steady-state and inflammatory DCs, but continuous Satb1 overexpression in differentiated DCs converts them into tolerogenic/pro-inflammatory cells that contribute to malignant progression.

INTRODUCTION

Special AT-rich binding protein 1 (Satb1) is a master genomic organizer that coordinates gene expression by forming loops in transcriptionally active chromatin (Cai et al., 2006; Yasui et al., 2002). Such loops bring enhancers and repressors separated by long sequences into close proximity with transcriptional start sites. Because both Satb1 and the DNA-binding zinc-finger protein CTCF associates with the nuclear matrix, it is likely that they interact to construct the appropriate higher-order chromatin structure (Lee and Iyer, 2012). Satb1 has been shown to regulate transcriptional programs by recruiting writers and erasers of histone modification (Cai et al., 2006; Pavan Kumar et al., 2006) and DNA methylation, as well as crucial transcription factors, including β-catenin (Notani et al., 2010). Satb1 therefore integrates global epigenetic and transcriptional programs that determine cellular phenotypes, differentiation, and activity of leukocyte subsets (Borghesi, 2014).

Recently, we found that *Satb1* is a direct target of *miR-155* in ovarian-associated dendritic cells (DCs) (Cubillos-Ruiz et al., 2012), which infiltrate solid ovarian tumors (Cubillos-Ruiz et al., 2009; Huarte et al., 2008; Scarlett et al., 2009, 2012). Although heterogeneity and phenotypic overlap complicate the categorization of myeloid subsets under inflammatory conditions (Segura and Amigorena, 2013), we demonstrated that when these leukocytes receive activating signals, they can effectively process and present antigens to T cells (Cubillos-Ruiz et al., 2009; Scarlett et al., 2009). However, in the absence of immunostimulatory interventions, tumor-associated DCs are spontaneously immunosuppressive (Scarlett et al., 2012). One recently identified mechanism driving the immunosuppressive phenotype of tumor-associated DCs is the constitutive activation of XBP1 (Cubillos-Ruiz et al., 2015). Regulatory ovarian cancer DCs express significant levels of CD86 and major histocompatibility complex class II (MHC II) and produce inflammatory pro-tumorigenic cytokines such as IL-6, CCL4, CXCL8, and CCL3 (Cubillos-Ruiz et al., 2009; Nesbeth et al., 2009; Scarlett et al., 2009). This phenotype matches the features of DCs indirectly activated by inflammatory cytokines in the absence of pattern recognition receptor stimulation (Joffre et al., 2009; Vega-Ramos et al., 2014).

To define the role of Satb1 in the differentiation of DCs in the steady state and cancer, we generated a conditional *Satb1*-deficient mice. Our results demonstrate that a dynamic pattern of Satb1 expression regulates the generation of conventional DCs as well as the acquisition of MHC II-dependent immunocompetence by inflammatory DCs through regulation of Notch signaling. However, unremitting expression in already differentiated DCs drives an inflammatory, immunosuppressive, and tumor-promoting phenotype.

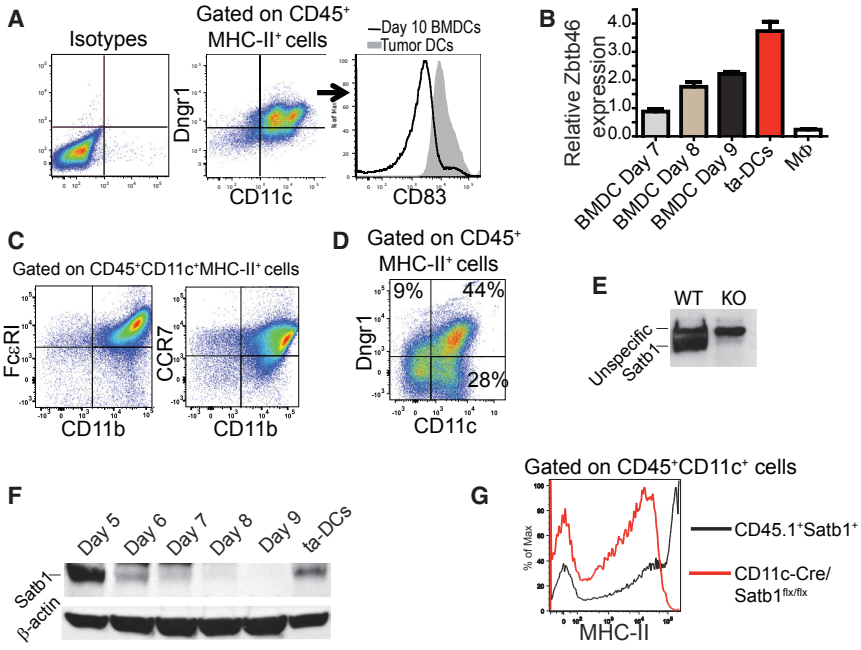

Figure 1. Activated Inflammatory DCs Infiltrate Syngeneic Ovarian Tumors in Mice

(A) $CD45^+CD11c^+MHC\ II^+$ cells in tumor ascites express Dngr1 and the activation marker CD83.

(B) *Zbtb46* transcript levels relative to *Gapdh* expression in $CD11c^+MHC\ II^+$ DCs in tumor ascites, total BMDCs at different stages of differentiation, and MHC $II^+F4/80^+$ splenic macrophages from tumor-free mice.

(C) Tumor-associated DCs express phenotypic markers of inflammatory DCs.

(D) $Dngr1^+CD11c^+MHC\ II^+$ DCs are also universally found in freshly dissociated orthotopic p53-driven ovarian tumors at days 62 after adenovirus-Cre-mediated activation of p53 and K-ras mutations. Representative of four different tumors analyzed.

(E) Western blot analysis of the thymus of wild-type and Satb1constitutive KO mice define the specificity of only the lower band.

(F) Western blot comparison of Satb1 expression in tumor-derived DCs versus BMDCs at different stages of differentiation.

(G) MHC II expression in tumor-derived ($CD45.2^+$) CD11c-Cre/$Satb1^{flx/flx}$ versus ($CD45.1^+$) wild-type $CD11c^+MHC\ II^+$ DCs in mixed BM chimeras challenged with ID8-*Defb29/Vegf-a* orthotopic tumors. Representative of three independent experiments.

RESULTS

Activated Inflammatory DCs Universally Infiltrate Solid Ovarian Tumors in Mice and Humans

We have previously demonstrated that supplementation of miR-155 to $CD11c^+DEC205^+MHC\ II^+$ leukocytes in the ovarian cancer microenvironment transforms them from an immunosuppressive to an immunostimulatory cell type through a mechanism involving silencing of Satb1 (Cubillos-Ruiz et al., 2009). To further define the phenotype of these cells in established, orthotopic ID8-*Defb29/Vegf-a* ovarian tumor-bearing mice, we used markers specifically expressed by bona fide DCs. As shown in Figure 1A, most $CD11c^+MHC\ II^+$ leukocytes in tumor ascites expressed the DC-specific lineage marker Dngr1 (Schraml et al., 2013). Tumor DCs also expressed the DC-specific transcription factor *Zbtb46* (Meredith et al., 2012; Satpathy et al., 2012), at levels comparable than $CD11c^+MHC\ II^+$ bone-marrow-derived DCs (BMDCs) and much higher than $F4/80^+MHC\ II^+$ macrophages in tumor-free mice (Figure 1B). Tumor-associated $CD11c^+MHC\ II^+Dngr1^+$*Zbtb46*$^+$ cells co-exhibited FcεRI, CD11b, and CCR7, phenotypic markers of inflammatory DCs (Segura and Amigorena, 2013). However, the expression of the DC lineage marker Dngr1 suggests that they are ontogenetically true DCs, rather than DC-like monocyte-derived cells (Figures 1A and 1C). An identical ($Dngr1^+$) phenotype was identified in tumor-associated DCs in orthotopic K-ras-driven solid ovarian carcinomas (Scarlett et al., 2012) (Figure 1D). Unexpectedly, DCs in tumor ascites also co-expressed the activation marker CD83 (Figure 1A). Therefore, although we have previously demonstrated that they primarily exert immunosuppressive activities (Cubillos-Ruiz et al., 2009, 2012; Huarte et al., 2008; Scarlett et al., 2009, 2012), bona fide DCs at ovarian cancer locations represent an activated cell type.

To define the role of Satb1 in tumor-associated DCs, we generated conditional *Satb1* knockout (KO) mice on a B6 background. We found that Abcam antibody #EPR3895 produced two clear bands. However, only the lower band at ~103 kDa disappeared in thymocytes from constitutive *Satb1* KO mice (Figure 1E) and therefore truly represented Satb1. More importantly, Satb1 expression levels in $CD11c^+MHC\ II^+$ DCs sorted from tumor ascites were significantly higher than in differentiated BMDCs, in which Satb1 expression starts decreasing coinciding with the transition to $CD11c^+MHC\ II^+$ from $CD11c^+MHC\ II^-$ precursors (days 5 and 6; Figure 1F). Supporting the role of Satb1 overexpression in mature tumor-associated DCs, congenic $Satb1^+$ DCs in tumor ascites exhibited higher levels of MHC II than their CD11c-Cre/$Satb1^{flx/flx}$ DCs in mixed bone marrow (BM) chimeras (Figure 1G).

Notably, the accumulation of bona fide DCs in ovarian mouse tumors recapitulates the immunoenvironment of human ovarian carcinomas, because $CD1c^+CD11c^+MHC\ II^+CD19^-CD70^{high}$ leukocytes (attributes of the human counterpart of inflammatory DCs; Segura and Amigorena, 2013; Segura et al., 2013) were found in all freshly dissociated solid advanced tumors samples analyzed (n = 12), at proportions ranging from 19% to 67% of total $CD45^+MHC\ II^+$ cells (Figures 2A and 2B). Tumor-infiltrating human DCs expressed levels of *ZBTB46* similar to their counterparts in matching peripheral blood or autologous monocyte-derived DCs (Figure 2C). As with their murine counterparts, despite showing relatively high expression of co-stimulatory molecules and MHC II, ovarian cancer-infiltrating DCs from three randomly selected patients did not elicit allogeneic responses, while autologous peripheral blood monocyte-derived DCs induced measurable proliferations (Figure 2D). Taken together, these results indicate that bona fide DCs universally

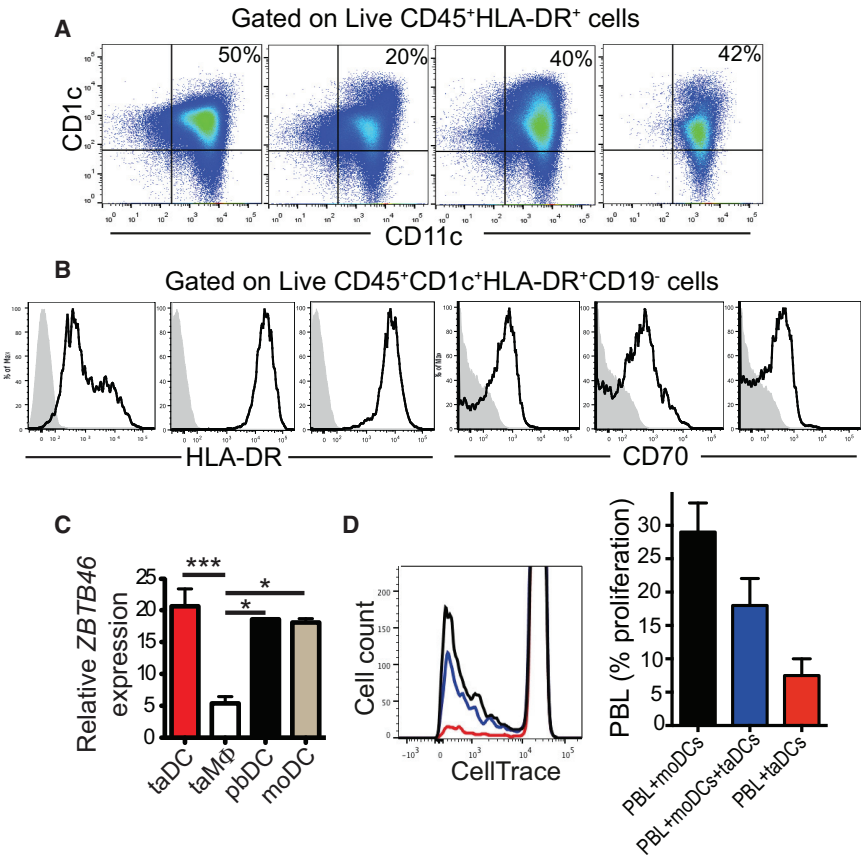

Figure 2. Inflammatory DCs Universally Infiltrate Solid Human Ovarian Carcinomas

(A) $CD45^+CD1c^+CD11c^+HLA\text{-}DR^+$ DCs in four different dissociated human ovarian carcinomas (representative of 12 tumors analyzed).

(B) Representative histograms of activation markers CD70 and HLA-DR in DCs infiltrating three different human ovarian carcinomas. Gray, isotype control used in each experiment. Representative of 12 different specimens analyzed.

(C) Zbtb46 mRNA expression relative to GAPDH expression in tumor-derived DCs ($CD45^+HLA\text{-}DR^+CD11c^+CD1c^+$), tumor-derived macrophages ($CD45^+HLA\text{-}DR^+CD11b^+CD1c^-$), peripheral-blood DCs ($CD45^+HLA\text{-}DR^+CD11c^+CD1c^+$), and monocyte-derived DCs from three patients.

(D) Representative mixed lymphocyte reaction assay performed by co-culturing matched-monocyte or tumor-derived DCs and allogeneic T cells (left). Proportions of allogeneic T cells proliferating in response to DCs from three different patients (right). All data represent mean ± SEM. $^*p < 0.05$, $^{***}p < 0.001$.

accumulate in the ovarian cancer microenvironment. Although Satb1 overexpression contributes to their activated phenotype, DC immunostimulatory function is severely abrogated at tumor locations.

Satb1 Governs the Generation and Maturation of Multiple Subsets of Conventional DCs

To understand the role of Satb1 in DC differentiation, we next performed competitive BM reconstitution experiments using BM from both constitutive and *Vav1*-Cre-driven *Satb1*-deficient mice. As shown in Figure 3A age-matched congenic wild-type and *Satb1* constitutive KO BM showed similar capacity to repopulate total leukocytes in the spleen and also a defect in the reconstitution of total DCs. Supporting previous reports (Alvarez et al., 2000), we observed a severe defect in T cell reconstitution in *Satb1*-deficient leukocytes (data not shown), compensated by the expansion of B cells (Figure 3B). We again found a reproducible decrease in the reconstitution of total splenic DCs arising from *Vav1*-Cre-*Satb1*$^{flx/flx}$ BM, compared to congenic wild-type progenitors, but this reduction selectively affected conventional (but not plasmacytoid) DCs (Figure 3C). *Satb1* deficiency also had divergent effects on different subsets of conventional DCs, causing a significant reduction of overall $CD4^+$ DCs in multiple experiments, while promoting the relative expansion of $CD11c^+CD4^-CD8^-B220^-$ DCs (Figure 3D). Interestingly, Satb1 ablation resulted in the elimination of a $CD103^+CD4^+$ subset, both in the steady state and upon DC mobilization induced by different cytokines (Figures 3D and 3E).

To dissect the role of Satb1 in the differentiation of antigen-presenting cells (APCs) generated under inflammatory conditions (Segura et al., 2013), we treated wild-type and *CD11c*-Cre/*Satb1*$^{flx/flx}$ BM with granulocyte-macrophage colony-stimulating factor (GM-CSF) in vitro. As shown in Figure 3F, left, the ablation of *Satb1* in lineage-committed BMDCs triggered by CD11c expression played no significant role in the acquisition of MHC I or cross-presentation of SIINFEKL to OT-1 CD8 T cells when differentiated $CD11c^+$ cells were pulsed with full-length ovalbumin (OVA) (Figure 3G, left). In contrast, only a small proportion of *Satb1*-deficient $CD11c^+$ cells acquired surface expression of MHC II (Figure 3F, right). Correspondingly, the same *Satb1*-deficient APCs that effectively presented antigen through class I failed to stimulate OT-II CD4 T cells (Figure 3G, right). In addition, Satb1-deficient APCs were unresponsive to Toll-like receptor (TLR)-mediated activation in terms of upregulation of MHC II and multiple co-stimulatory molecules (Figure 3H). Together, these experiments indicate that Satb1 plays divergent roles in the differentiation of conventional DC subsets and contributes to expression of MHC II during inflammatory APC differentiation and TLR-dependent increase of co-stimulatory molecules.

Satb1 Drives the Expression of MHC II on Inflammatory DCs through a Transient Notch-Signaling-Dependent Transcriptional Mechanism

Supporting a transcriptional defect, we found significantly lower H2-Ab1 mRNA levels in APCs generated in the absence of Satb1 (Figure 4A). Similar transcriptional differences were obtained with sorted $CD11c^+CD135^+CD115^-$ cells, specifically derived

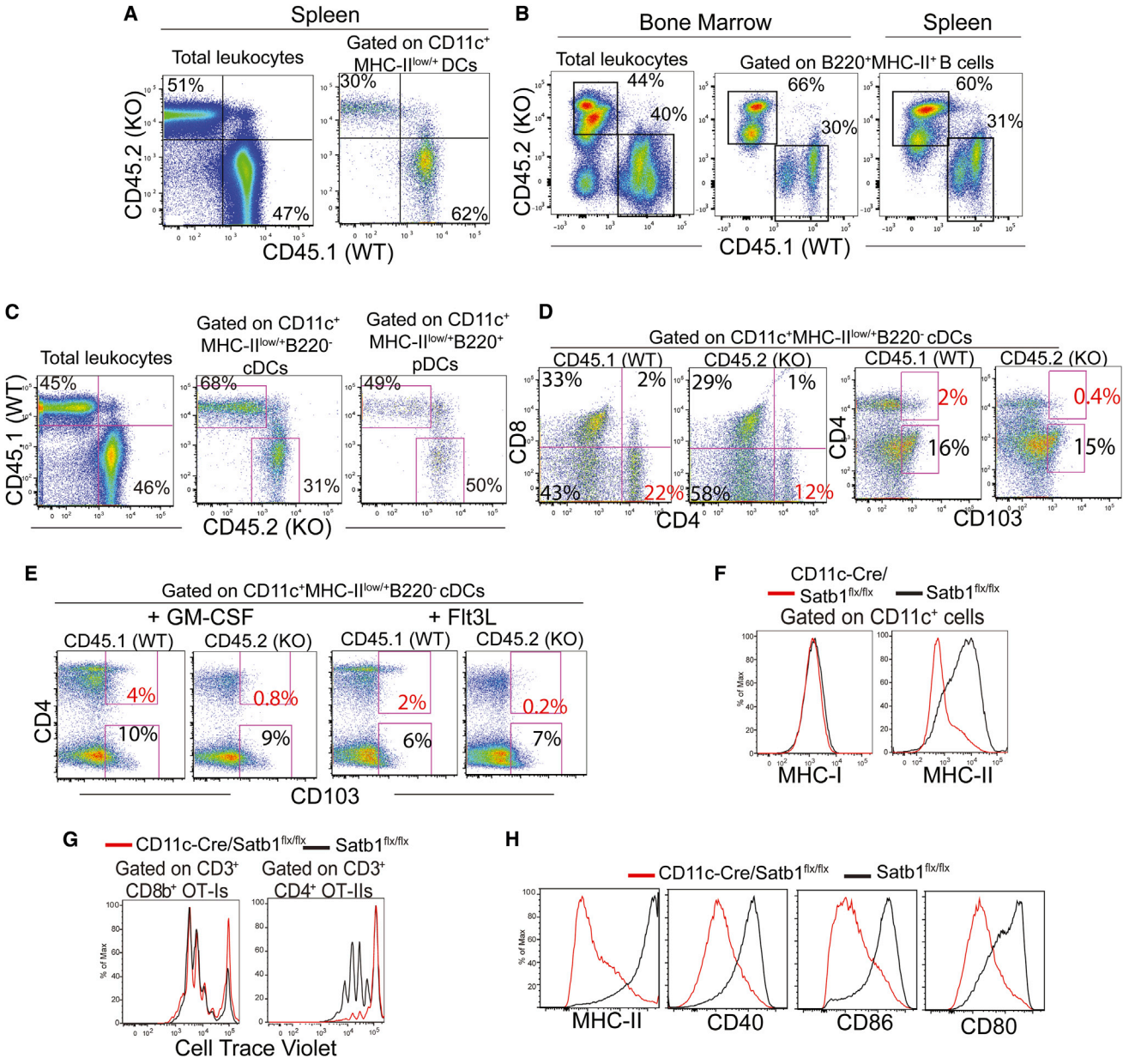

Figure 3. Satb1 Influences the Generation and Maturation of Conventional DCs

(A) Mice reconstituted with equal proportions of age-matched wild-type (CD45.1) and constitutive Satb1-deficient BM (CD45.2) analyzed ~2 months after reconstitution.

(B and C) Analysis of spleens from mixed BM chimeras ~2 months after competitive reconstitution with equal ratios of adult age-matched wild-type (CD45.1) and Vav1-Cre/*Satb1*$^{flx/flx}$ (CD45.2) BM. Representative of three or more independent experiments with seven or more mice/group.

(D) Reduction of *Satb1*-deficient total CD4$^+$ and CD4$^+$CD103$^+$ conventional DCs with concomitant expansion of CD4$^-$CD8$^-$ subsets in the spleen of mixed wild-type/Vav1-Cre/*Satb1*$^{flx/flx}$ BM chimeras.

(E) Ablation of *Satb1*-deficient CD4$^+$CD103$^+$ conventional DCs in response to intraperitoneal administration of Flt3L (10 μg/mouse) and GM-CSF (5 μg/mouse) for 5 consecutive days to induce DC mobilization. Both representative of two or more independent experiments and readouts at day 6.

(F) MHC I and MHC II expression in (CD45.1$^+$) wild-type and (CD45.2$^+$) CD11c-Cre/*Satb1*$^{flx/flx}$ BMDCs co-cultured for 8 days in the presence of GM-CSF. Representative of three independent experiments.

(G) Wild-type and CD11c-Cre/Satb1$^{flx/flx}$ BMDCs differentiated for 8 days were pulsed with full-length ovalbumin and incubated with Cell Trace Violet-labeled OT-I or OT-II T cells. Representative of three independent experiments.

(H) Expression of co-stimulatory markers in (day 9) wild-type and CD11c-Cre/Satb1$^{flx/flx}$ BMDCs after 18 hr incubation with 1 μg/ml lipopolysaccharide.

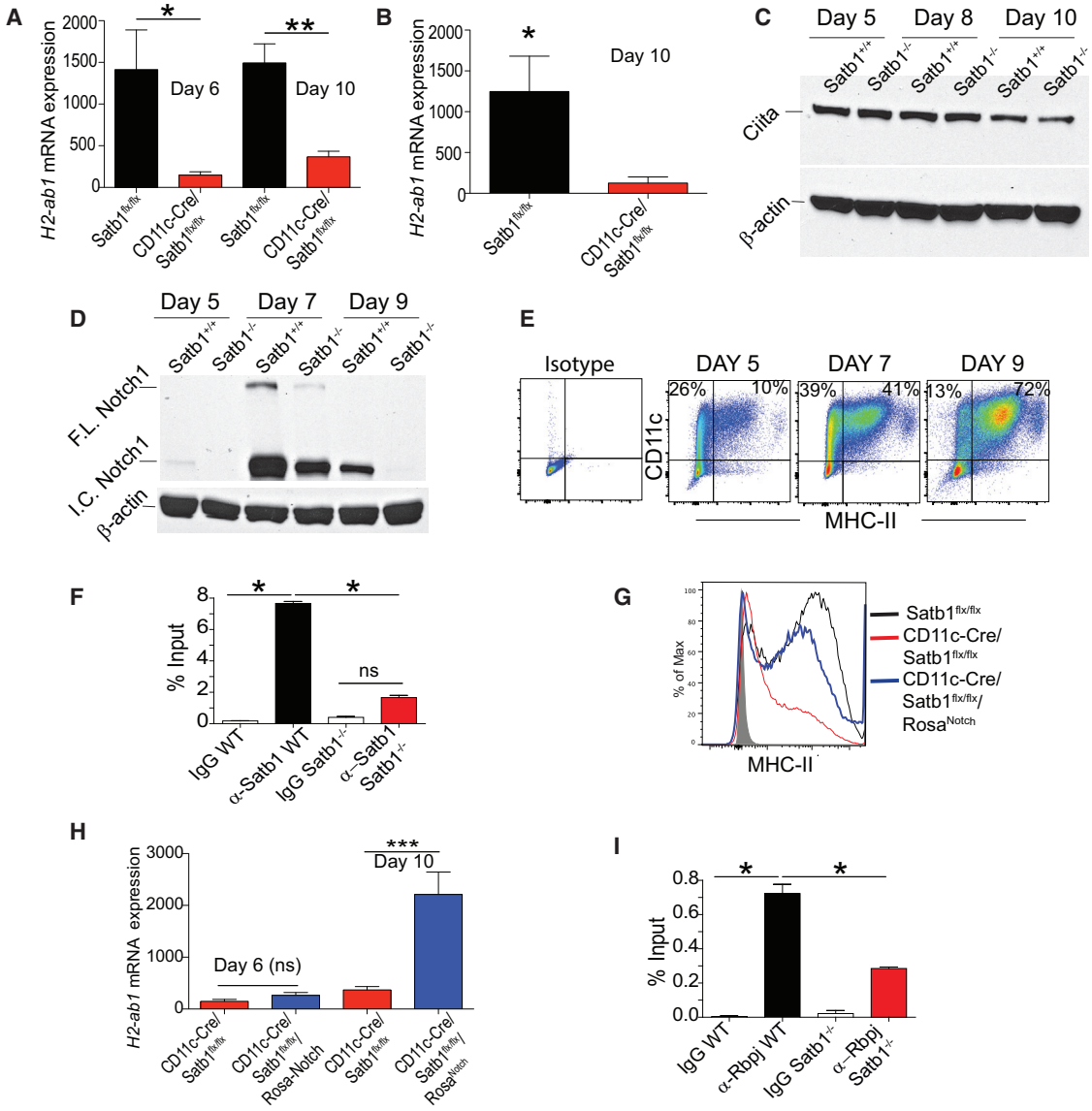

Figure 4. Satb1 Drives the Expression of MHC II on the Surface of Differentiated DCs by Regulating Notch1 Signaling

(A) Quantification of *H2-Ab1* transcripts relative to *Gapdh* expression at days 6 and 10 of GM-CSF-induced DC differentiation from *Satb1*$^{flx/flx}$ and CD11c-Cre/ *Satb1*$^{flx/flx}$ BM. Representative of three experiments in triplicate.

(B) qPCR quantification of *H2-Ab1* mRNA in CD11c^{+}CD135^{+}CD115^{-} cells sorted after 10 days of GM-CSF-induced DC differentiation as in (A). Representative of two experiments in triplicate.

(C) Ciita expression in *Satb1*$^{flx/flx}$ and CD11c-Cre/*Satb1*$^{flx/flx}$ BMDCs at different times of GM-CSF-induced differentiation. Representative of three experiments.

(D) Expression of full-length and intracellular Notch1 during GM-CSF-induced DC differentiation of BM from *Satb1*$^{flx/flx}$ and CD11c-Cre/*Satb1*$^{flx/flx}$. Representative of three independent experiments.

(E) Dynamics of GM-CSF-induced differentiation of wild-type CD11c^{+}MHC II^{+} BM cells in these cultures.

(F) Satb1 binding to the Notch1 promoter. Chromatin was immunoprecipitated with anti-Satb1 antibodies (Abs) or control immunoglobulin G (IgG) from CD11c^{+}APCs differentiated for 7 days with GM-CSF, derived from the BM of wild-type (WT) versus CD11c-Cre/ *Satb1*$^{flx/flx}$ (KO; control) mice. Enrichment of the Notch1 promoter sequence in chromatin immunoprecipitated with anti-Satb1 Abs versus irrelevant IgG was quantified by real-time qPCR. Representative of two independent experiments in triplicate, with similar results.

(G) MHC II expression in CD45^{+}CD11c^{+} BM cells from either *Satb1*$^{flx/flx}$, CD11c-Cre/*Satb1*$^{flx/flx}$ or Rosa^{Notch} mice differentiated with GM-CSF. Representative of three independent experiments.

(H) Quantification of *H2-Ab1* transcripts relative to *Gapdh* expression at days 6 and 10 of GM-CSF-induced DC differentiation from CD11c-Cre/*Satb1*$^{flx/flx}$ and Rosa^{Notch} BM. Representative of three experiments.

(I) qPCR of CD11c^{+} APCs as described above for *H2-ab1* promoter sequences in chromatin immunoprecipitated with anti-Rbpj Abs versus irrelevant IgG. Representative of two independent experiments in triplicate, with comparable results. All data represent mean ± SEM.*$p < 0.05$, **$p < 0.01$, and ***$p < 0.01$.

from Dngr1$^+$ DC precursors (Helft et al., 2015) (Figure 4B). Surprisingly, we found no Satb1-dependent differences in the expression levels of Ciita, which controls MHC II transcription by associating with the basal transcription machinery (Lochamy et al., 2007) (Figure 4C).

To identify Satb1-dependent regulators of MHC II expression, we focused on Notch1. Although Notch1 signaling is typically associated with lymphocytic differentiation, recent studies indicate that Delta-like1-signaling drives cell surface expression of MHC II in mast cells (Nakano et al., 2009). Accordingly, we found that at days 6–7 of GM-CSF-differentiation of wild-type BM, precisely coinciding with the upregulation of MHC II in CD11c$^+$ cells, Notch expression is elevated in immature myeloid cells and is progressively downregulated upon terminal differentiation of APCs (Figures 4D and 4E). This occurs in a Satb1-dependent manner, because a significant decrease in both full-length and intracellular Notch1 was identified in nascent APCs upon CD11c-induced ablation of *Satb1*.

To determine whether Satb1 physically associates with the Notch1 promoter, we performed chromatin immunoprecipitation (ChIP) with specific antibodies, using *Satb1*$^{-/-}$ APCs as a control. As shown in Figure 4F, we observed significant enrichment of the Notch1 promoter in Satb1-DNA precipitates from day 7 BM-derived CD11c$^+$MHC II$^+$ APCs, compared to control pull-downs with an irrelevant immunoglobulin G. Supporting the specificity of the binding to the Notch1 promoter, no significant enrichment was found in identically differentiated APCs from *CD11c*-Cre/*Satb1*$^{flx/flx}$ mice (Figure 4F).

Next, we generated triple (*CD11c*-Cre/*Satb1*$^{flx/flx}$/Rosa^{Notch}) transgenic mice and brought them to a B6 background. In this system, CD11c expression triggers Satb1 ablation while simultaneously driving the expression of intracellular (constitutively activated) Notch1 (Murtaugh et al., 2003) during GM-CSF-induced differentiation of BM cells into APCs. Supporting the role of Notch signaling in MHC II transcription, Cre-mediated Notch activation restored cell-surface expression of MHC II (Figure 4G) by upregulating *H2-Ab1* mRNA levels (Figure 4H). Finally, we observed significant enrichment of *H2-ab1* promoter sequences in Rbpj-DNA precipitates (but not Hes1-DNA precipitates; data not shown), indicating that Notch signaling turns on MHC II through transcriptional activation (Figure 4I). As expected, Rbpj occupancy of the *H2-ab1* promoter decreased significantly in APCs (Figure 4I). Together, our results unveil a mechanism whereby Satb1 drives the expression of Notch in APC precursors (including bona fide pre-DCs) by directly activating the promoter. By governing MHC II transcription, Notch signaling drives cell-surface expression of MHC II during APC differentiation, licensing them for antigen presentation.

Silencing Satb1 in Tumor-Associated DCs Boosts Anti-tumor Immunity and Delays Malignant Progression

The aforementioned results indicate that Satb1 is required for full DC differentiation and MHC II-dependent T cell stimulatory activity. Correspondingly, *CD11c*-Cre/*Satb1*$^{flx/flx}$ BM-reconstituted mice succumbed to tumor challenge significantly faster than wild-type BM-reconstituted controls, suggesting that DCs were incapable of orchestrating protective immunity (Figure 5A).

To reconcile the overexpression of Satb1 in tumor DCs with their immunosuppressive phenotype, we focused on the fact that, unlike tumor-associated DCs, BMDCs downregulate Satb1 after maturation (Figure 1F). We found that inflammatory factors such as S100A8/A9 were sufficient to further upregulate Satb1 in vivo in DCs in the tumor microenvironment (TME), while estrogen signaling had the opposite effect (Figure 5B). To define the effect of inflammation-induced Satb1 overexpression in *already differentiated* DCs (as opposed to DC precursors), we silenced *Satb1* specifically in tumor-associated DCs using small interfering RNA (siRNA)-carrying nanoplexes. Polyethylenimine (PEI)-based nanoparticles carrying fluorescently labeled siRNA were selectively engulfed by CD11c$^+$ leukocytes at peritoneal (ID8-*Defb29*/*Vegf-a* tumor) locations, as we reported (Cubillos-Ruiz et al., 2009, 2012) (Figure 5C). *Satb1*-targeting, but not control (non-targeting), nanoparticles effectively silenced *Satb1* expression in vivo in ovarian cancer DCs (Figure 5D) and, accordingly, induced Notch1 downregulation. Most importantly, silencing *Satb1* throughout the course of malignant progression significantly enhanced anti-tumor immunity, as determined by both Granzyme B and IFN-γ ELISPOT analysis (Figure 5E). Accordingly, the accumulation of antigen-experienced (CD44$^+$) cytotoxic T cells exhibiting markers of recent activation was also significantly increased upon *Satb1* silencing (Figure 5F). Furthermore, OT-I T cells responded significantly more strongly to cognate antigen in situ in the ovarian cancer microenvironment when *Satb1*-silenced tumor DCs were pulsed in vivo with full-length OVA, compared to DCs identically pulsed in mice treated with irrelevant nanoparticles (Figures 5G and 5H). Supporting the relevance of enhanced protective immunity, repeated *Satb1* silencing specifically in DCs resulted in significantly longer survival rates, compared to control irrelevant siRNA nanocomplexes (Figure 5I). Therefore, inflammatory cytokines in the TME upregulate *Satb1*, resulting in an immunosuppressive, tumor-promoting phenotype.

Satb1 Governs Genome-wide Transcriptional Modifications

To define the spectrum of transcriptional changes induced by Satb1 overexpression, we treated mice with ovarian cancer-induced ascites with fluorescently labeled Satb1-specific versus non-targeting PEI-based nanocomplexes. After 20–24 hr, CD11c$^+$MHC II$^+$ DCs targeted by functional Satb1-specific or identically delivered control siRNA were collected and subjected to RNA deep-sequencing. In the first experiment, mRNA of *Satb1* was reduced 4.8-fold and overall, 1,003 genes changed their expression by at least 50% (Data S1). In the second experiment, when Satb1 reduced expression only by 20%, we found 521 genes that significantly changed expression with any fold (Data S1). Significant overlap between the two sets of 72 genes (Figure 6A, $p = 3 \times 10^{-11}$ by hypergeometric test) indicates that there is a subset of genes sensitive to Satb1 expression even when the expression changes are very small. The full list of 72 genes significantly up- and downregulated with any level of *Satb1* changes in both experiments, which includes an array of inflammatory cytokines and chemokines, is shown in Figure 6B.

In addition, Ingenuity Pathway Analysis of the 1,003 genes that underwent expression change of at least 1.5-fold upon Satb1

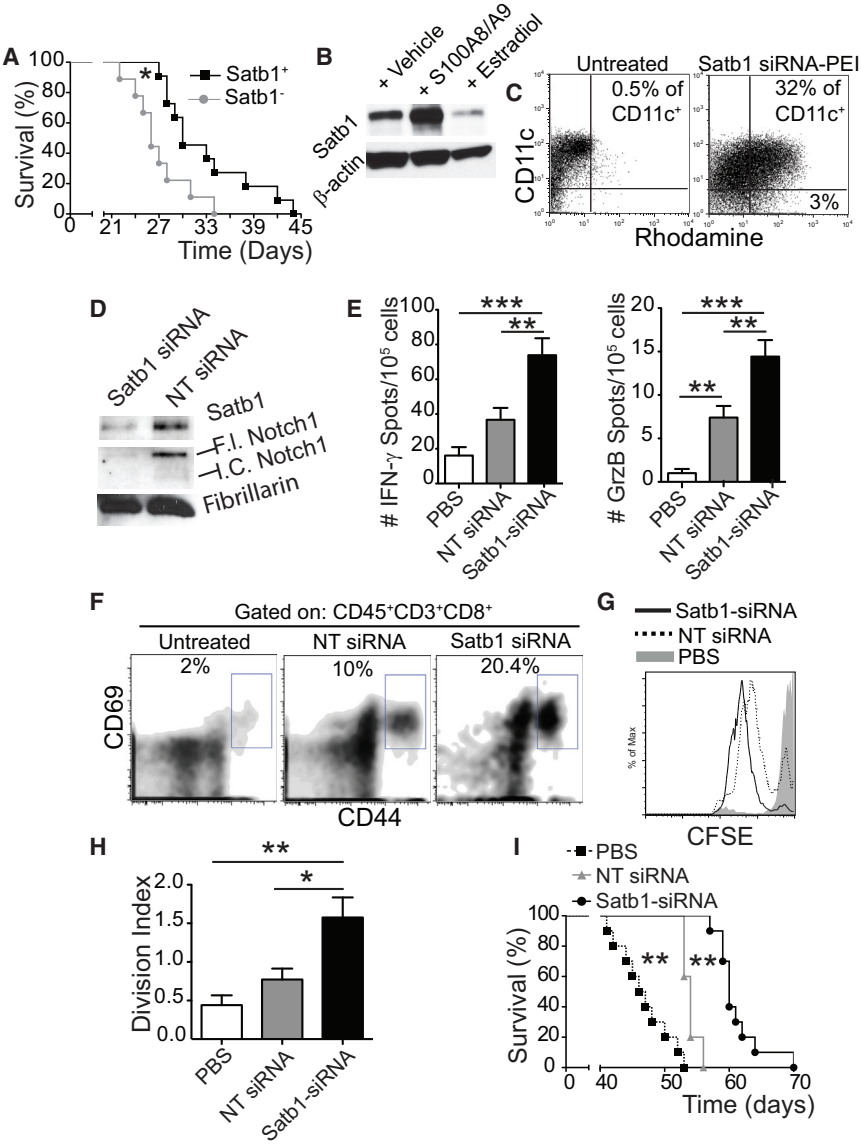

Figure 5. Silencing Satb1 in Tumor-Associated DCs Boosts Anti-tumor Immunity and Delays Malignant Progression

(A) Survival of mice reconstituted with wild-type versus CD11c-Cre/*Satb1*$^{flx/flx}$ BM after ID8-*Defb29*/*Vegf-a* tumor challenge. Two independent experiments pooled (9–10 mice/group).

(B) Mice bearing ID8-*Defb29*/*Vegf-a* tumor ascites received S100A9 (25 μg) or β-estradiol (0.01 mg) i.p. CD11c^{+}MHC II^{+} DCs were FACS-sorted and analyzed for Satb1 expression 34–48 hr later. Representative of three independent experiments.

(C) Rhodamine-labeled Satb1-targeting siRNA-PEI nanoparticles were i.p. injected into 3-week ID8-*Defb29*/*Vegf-a* tumor-bearing mice. Rhodamine^{+} DCs were identified ~36 hr later.

(D) Satb1 and Notch1 expression in CD11c^{+}MHC II^{+} DCs sorted from tumor ascites ~36–48 hr after i.p. administration of non-targeting (NT) or *Satb1*-targeting siRNA-PEI (F.l., full-length, I.C., intracellular).

(E and F) Mice received indicated treatments at days 8, 13, 18, 23, and 28 after tumor challenge. T cells from ascites were used for IFN-γ- and Granzyme B-ELISPOT analysis (E) or expression of CD44 and CD69 levels (F). Representative of two independent experiments (four to six mice per group).

(G) ID8-*Defb29*/*Vegf-a* tumor-bearing mice treated for 3 weeks with siRNA-carrying nanocomplexes or PBS received 0.6 mg full-length endotoxin-free ovalbumin i.p. 3 hr after the last treatment, followed 18 hr later by i.p. transfer of 2 ± 10^{6} carboxyfluorescein succinimidyl ester (CFSE)-labeled SIINFEKL-specific OT-1 T cells. Peritoneal wash was collected after 48 hr and CFSE dilution was quantified. Representative of three independent experiments (six mice per group).

(H) Division Index of proliferating cells in (F).

(I) ID8-*Defb29*/*Vegf-a* tumor-bearing mice received five treatments every 5 days and were monitored for survival. Data represent two independent experiments with ten mice total per group. All data represent the mean ± SEM. *p < 0.05, **p < 0.01, and ***p < 0.001.

silencing of 4.8-fold in tumor-associated DCs revealed many signaling pathways affected in *Satb1*-overexpressing cells (Figure 6C). Inflammatory networks driven by *Satb1* overexpression included *Il6*-mediated pathways and pathways for granulocyte and agranulocyte adhesion and diapedesis. Upstream regulator analysis revealed multiple regulators affected by *Satb1* (Figure 6D) as estimated from mRNA changes in their known targets. For example, *Ifnb1* and *Tnf*, in which mRNA levels were most significantly altered, were indeed functionally more active with *Satb1* overexpression, as 38 targets for *Ifnb1* and 139 targets for *Tnf* displayed significant mRNA changes, indicative of the regulators' activation.

In accordance with results of pathway analysis, *Il6* target genes demonstrated that *Il6* was more active when *Satb1* was present. Supporting our in vitro results, we also observed similar effects on *Notch1* signature and, interestingly, an *Lgals1* signature. Galectin-1, encoded by the *Lgals*1 gene, is a pleiotropic protein that binds to surface glycoconjugates containing N-acetyllactosamine sequences, cross-linking these saccharide structures on immune cells and driving potent immunosuppression (Dalotto-Moreno et al., 2013; Rubinstein et al., 2004; Rutkowski et al., 2015; Toscano et al., 2007). Together, these data indicate that unremitting overexpression of *Satb1* in already differentiated inflammatory DCs in the TME drives genome-wide transcriptional changes that globally affect the transcriptome and promotes an immunosuppressive phenotype.

Satb1-Dependent Secretion of Galectin-1 Is Sufficient to Accelerate Tumor Progression

Substantiating the relevance of our genomic analysis, fluorescence-activated cell sorting (FACS)-sorted DCs engulfing Satb1-silencing nanocomplexes secreted significantly lower

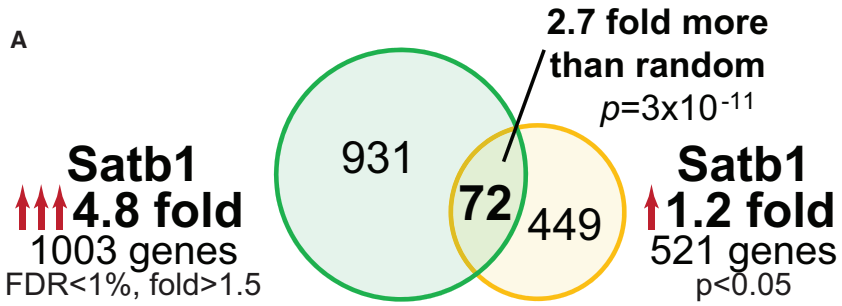

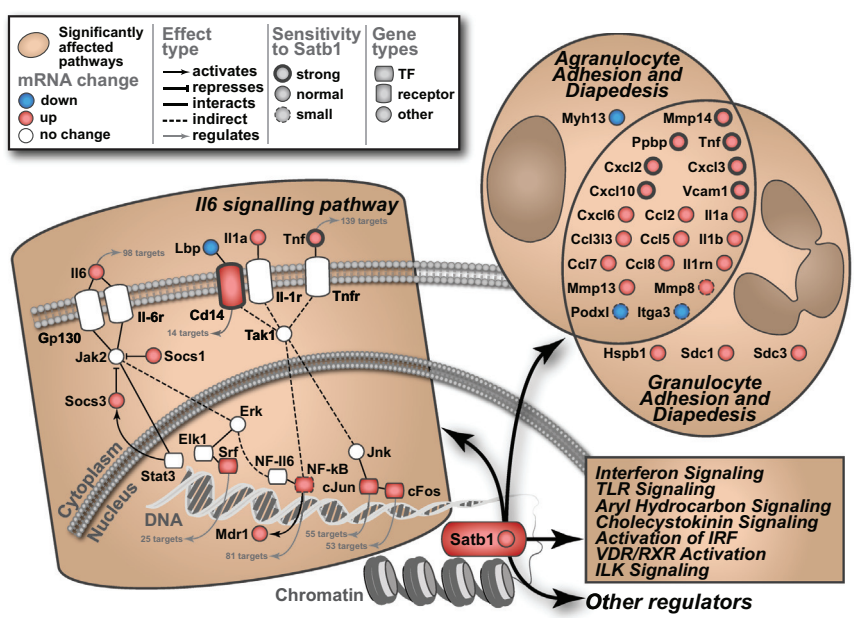

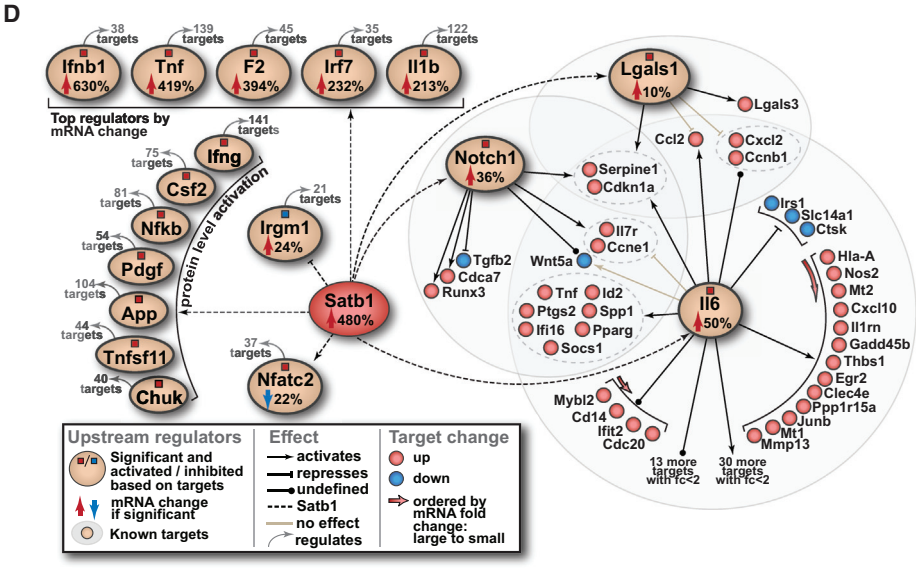

B

max N/S fold	↑↑↑4.8 NT 1	↑↑↑4.8 NT 2	↑↑↑4.8 Satb1 1	↑↑↑4.8 Satb1 2	↑1.2 N 1	↑1.2 S 1	Satb1 / Genes
12							Upp1
4.4							Fam71a
4.2							Tnf
10							Cxcl3
5							Cxcl2
3.4							Cxcl1
3.7							Mt2
3							Procr
3.4							Irg1
3							Cxcl10
4.5							Efr3b
4.6							Ptgs2
4.1							Tarm1
2.8							Tnfaip3
3.3							Selenbp1
3.1							Ppbp
2.7							2310016C08Rik
3.4							Niacr1
5.6							Slpi
2.8							Pira6
2.6							Gdf15
2.4							Rsad2
2.7							Serpine1
2.4							Egr1
2.7							Cd14
2.9							Ier3
2.5							Ets2
4.3							Slc7a11
2.3							Mxd1
4.3							Adm
2.6							Pde4b
3.4							Slc2a6
3							Mmp14
2.4							Vcam1
2.7							Slc2a1
2.6							Ccrl2
-3.6							Plcb4
-4.4							Sspn
-2.7							Smarca2
-5.9							Rspo1
-5.1							Irs1
-4.4							Eppk1
-4.4							Zfpm2
-5.6							Scrn1
-4.4							Dlg5
-3.7							Ldhb
-6.4							Kirrel
-4.7							Dock9
-4.7							Gpr125
-4.2							Fxyd3
-2.8							Cpe
-3.6							Cacna2d1
-4.9							Etl4
-5.3							Mtap1b
-4.5							Nfib
-4.7							Gpx8
-3.3							Rab6b
-3.8							Cyp1b1
-5.2							Gpr56
-4							mKIAA1011
-3.5							Neo1
-4.4							Aox3
-3.8							Dsp
-6.2							Crb2
-4.5							Arhgap42
-5.3							Wnt5a
-3.4							Ltbp4
-6.9							Gna14
-11							Cadm3
-4.1							Gpc4
-5.5							Cyp26b1
-5.3							Mapk8ip1

(legend on next page)

levels of both IL-6 and galectin-1, compared to non-targeted siRNA-untreated controls (Figure 7A). Correspondingly, enforced retroviral-mediated expression of Satb1 augmented their production of both galectin-1 and tumor-promoting IL-6 (Figure 7B).

We have previously identified galectin-1 as a major pathogenic factor in a variety of tumors (Rutkowski et al., 2015). To determine the relevance of Satb1-dependent upregulation of galectin-1 specifically in tumor microenvironmental DCs, we ectopically overexpressed Satb1 in wild-type and galectin-1-deficient BMDCs, independently admixed them with tumor cells, and used the mixture to challenge different cohorts of naive mice. As shown in Figures 7C and 7D, these slowly progressing tumors grew significantly faster when admixed with Satb1-overexpressing wild-type DCs, compared to mock-transduced control DCs. However, Satb1-dependent acceleration of tumor growth (versus the administration of tumor cells without DCs) only occurred when tumor-associated DCs had the capacity to upregulate galectin-1 (Figure 7C). Importantly, galectin-1-deficient BMDCs showed the same differentiation kinetics as their wild-type counterparts (Figure 7E). Similarly, when tumor cells were admixed with *Satb1*-transduced IL-6$^{-/-}$ DCs, they still grew significantly faster than tumors containing mock-transduced IL-6$^{-/-}$ DCs, but significantly more slowly than tumors admixed with *Satb1*-transduced wild-type DCs (Figures 7F and 7G). Together, these results indicate that Satb1 unrelenting overexpression drives complex tumor-promoting, pro-inflammatory activities in tumor-associated DCs, for which the secretion of immunosuppressive galectin-1 and IL-6 are significant contributors.

DISCUSSION

We find that Satb1 governs a genome-wide transcriptional program required for terminal steady-state DC differentiation and effective antigen presentation through MHC II. Paradoxically, Satb1 needs to be extinguished after DC maturation for effective immunostimulatory activity. Accordingly, unremitting expression of Satb1 in fully committed inflammatory DCs in solid ovarian tumors drives an immunosuppressive cell type that outnumbers canonical macrophages and contributes to accelerate malignant progression.

Inflammatory TLR signals appear to be necessary to activate DCs for effective T cell priming, but cytokines such as interleukin 1β (IL-1β), tumor necrosis factor (TNF), or type I interferons can activate DCs in an alternative manner. Although these inflammatory cytokines induce DC maturation, they are not sufficient to generate T cell stimulatory DCs. Thus, DCs that were activated by cytokines in the absence of TLR agonists do not efficiently prime effector T cell responses and are regarded as poor stimulators of T cell-mediated immunity (Joffre et al., 2009). Inflammation, therefore, does not substitute for pattern recognition receptor signaling, but it does alter the nature and magnitude of cytokines secreted by DCs. Cytokine-activated DCs, for instance, produce much higher amounts of IL-6, CCL3, or CCL4 in response to TLR activation, compared to their immature counterparts (Vega-Ramos et al., 2014).

Unlike other tumors that accumulate immature myeloid progenitors but few mature DCs, we have previously identified activated bona fide inflammatory DCs as an abundant population in the microenvironment of solid ovarian carcinomas (Cubillos-Ruiz et al., 2009; Huarte et al., 2008; Scarlett et al., 2009, 2012). Their DC nature is supported by the expression of *Zbtb46* transcripts (Meredith et al., 2012; Satpathy et al., 2012). Additionally, ovarian cancer DCs can be induced to process full-length OVA in vitro (Conejo-Garcia et al., 2004) and in vivo (Cubillos-Ruiz et al., 2009; Scarlett et al., 2009) to present processed SIINFEKL to T cells. Although inflammatory DCs are thought to originate from monocytes (Segura and Amigorena, 2013), murine ovarian cancer DCs express the DC lineage marker Dngr1 (Schraml et al., 2013), suggesting that they may alternatively arise from DC precursors. Their mature phenotype suggests a role for indirect inflammatory activation in the acquisition of a tumor-promoting phenotype by ovarian-cancer-associated DCs (Huarte et al., 2008; Scarlett et al., 2012). Supporting this proposition, we found that S100A8/A9 proteins upregulate Satb1 in DCs in vivo and in vitro and that Satb1 expression enhances the secretion of inflammatory cytokines and chemokines by DCs. Accordingly, silencing *Satb1* expression selectively in tumor-associated DCs in vivo at tumor locations reduced the level of inflammation and immunosuppression in the TME and boosted T cell-mediated immune protection. Notably, 22% of transcripts underwent ≥2-fold changes in expression levels upon Satb1 knockdown. Therefore, consistent with its role as a master genomic organizer, Satb1 drives major phenotypic changes that are sufficient to accelerate malignant progression and suppress anti-tumor immunity. Although this study cannot segregate the precise contribution of Satb1-dependent loop formation to the entire range of genome-wide effects, it is likely that these dramatic phenotypic changes are the result of both looping and transcriptional activator/repressor activities. Of note, although Satb1 is highly similar to Satb2 and both regulate chromatin remodeling and gene regulation, the latter is not expressed in BMDCs (not shown), and therefore all observed effects can only be attributed to Satb1.

Among the spectrum of Satb1-dependent mechanisms, we identified the direct activation of the Notch1 promoter as a driver

Figure 6. Transcriptional and Regulatory Changes Caused by Satb1 Overexpression

(A) Numbers of significantly changed genes and their overlap between two independent experiments that changed expression of *Satb1* 4.8-fold and 1.2-fold. The overlap was 2.7 more than expected by random chance alone ($p = 3 \times 10^{-11}$ by hypergeometric test).

(B) Expression heatmap and fold changes for 72 genes affected by high and low levels of Satb1 change. N and NT indicate NT siRNA-treated samples, and S and *Satb1* indicate *Satb1*-siRNA treated samples.

(C) Canonical pathways significantly affected by *Satb1* overexpression. *Il6*-mediated pathways and pathways for granulocyte and agranulocyte adhesion and diapedesis were among the most significantly affected and were highlighted to demonstrate expression changes of individual genes in the pathway.

(D) Predicted upstream regulators whose regulatory function was significantly affected by *Satb1* as evidenced by mRNA expression changes of their known target genes.

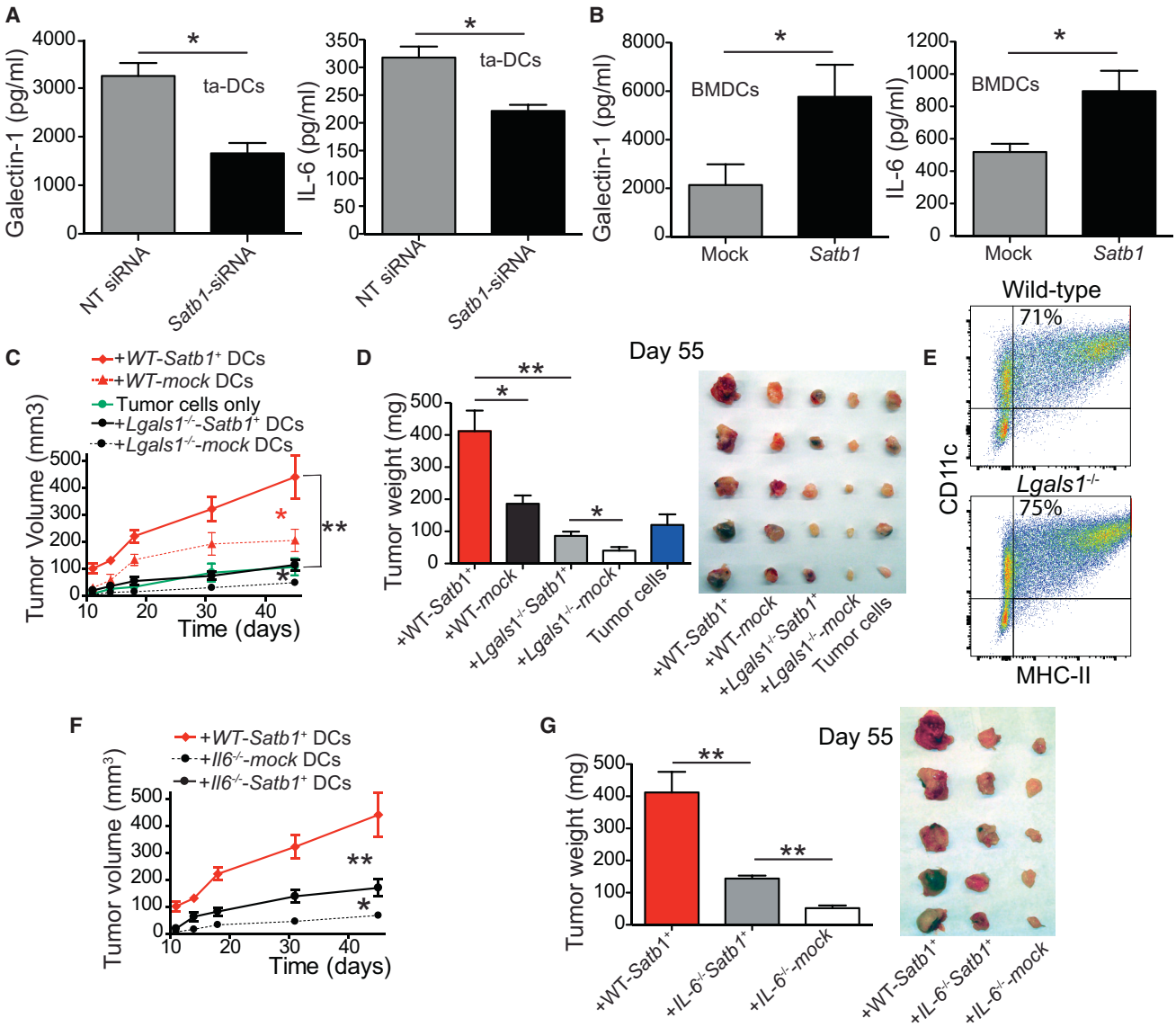

Figure 7. Satb1 Overexpression of Tumor DCs Accelerates Malignant Progression by Promoting the Secretion of IL-6 and Galectin-1

(A) ELISA quantification of galectin-1 and IL-6 released by phorbol 12-myristate 13-acetate (PMA)/ionomycin (500 ng/1 μg/ml)-stimulated CD11c+MHC II+ DCs sorted from ~day 35 tumor ascites, 20–24 hr after treatment with 100 μg of Rhodamine-labeled NT or Satb1-targeting siRNA-carrying polyplexes. Pooled from two independent experiments.

(B) GM-CSF-differentiated wild-type BM cells were transduced at days 2 and 3 with empty or Satb1-encoding retroviruses. Galectin-1 and IL-6 quantified in supernatants of PMA/ionomycin-stimulated mock- or Satb1-transduced BMDCs. Pooled from two independent experiments in triplicate.

(C) Wild-type and Lgals1$^{-/-}$ BMDCs were transduced with Satb1 or the empty retrovirus and admixed (1:10 ratio) with 106 ID8-Defb29/Vegf-a cells for injection into the axillary flank. Tumor growth was monitored. With the exception of tumor cells alone and mock transduced Lgals1$^{-/-}$ DCs, representative of three independent experiments (five or more mice per group).

(D) Tumor weight and size comparison of tumors resected at day 55 in one of the experiments.

(E) Comparable proportions of CD11c+MHC II+ DCs generated from wild-type and Lgals1$^{-/-}$ BM after 9 days of culture with GM-CSF. Representative of three independent experiments.

(F) Mice (5/group) were challenged with ID8-Defb29/Vegf-a tumors admixed with Satb1/mock-transduced wild-type versus Il6$^{-/-}$ BMDCs as in (C), and tumor growth was monitored.

(G) Tumor weight and size comparison of tumors resected at day 55. All data represent the mean ± SEM. *p < 0.05, **p < 0.01, and ***p < 0.001.

of terminal inflammatory DC differentiation. Notch1 is transiently upregulated during the switch from CD11c^{+}MHC II^{-} to CD11c^{+}MHC II^{+} APCs. Using genetically engineered systems, our data indicate that ectopic expression of Notch is sufficient to restore MHC II surface expression in the absence of Satb1, through a transcriptional mechanism dependent on direct

binding of Rbpj to the *H2-Ab1* promoter. Although seminal studies by the Gabrilovich lab had previously identified a role for Notch in DC differentiation (Zhou et al., 2009), the requirement of Notch signaling for the acquisition of MHC II immunocompetence in inflammatory DCs is surprising and opens avenues to understanding how transient Notch signaling could contribute to emergency myelopoiesis.

Finally, our study identifies galectin-1, an immunosuppressive lectin, as a major target of Satb1 in tumor-associated DCs. As galectin-1 coordinates tolerogenic programs in human and mouse DCs (Ilarregui et al., 2009), limits survival of Th1 and Th17 cells (Toscano et al., 2007), and promotes the differentiation of tumor Foxp3$^+$ T regulatory cells (Dalotto-Moreno et al., 2013), our findings suggest that Satb1 may contribute to tumor progression by hierarchically activating galectin-1-driven cancer immune-evasive pathways. The dramatic effect that Satb1-dependent, DC-derived galectin-1 production in nascent tumors has on subsequent tumor growth supports the relevance of this mechanism. Overall, our results show an alternative Satb1-driven mechanism that controls DC function in healthy conditions and cancer.

EXPERIMENTAL PROCEDURES

Mice and Cell Lines

Satb1 transgenic mice used in this work were generated by Wistar's Mouse Transgenic Facility with clones of embryonic stem cells carrying a targeted/floxed version of Satb1 procured from EUCOMM and injected into blastocysts. The resulting heterozygous colony founders were crossed with C57BL/6 breeders to confirm parental transmission of the targeted version of Satb1, genotyped for *loxP* and LacZ and further crossed until homozygosis to obtain a *Satb1* full KO mice. Complete absence of Satb1 expression in Satb1 KO mice was verified by western blot in the thymus, an abundant source of Satb1 expression. To be able to specifically ablate Satb1 expression in certain cell compartments, *Satb1*$^{floxed/wt}$ mice were crossed with the deleter strain ACTFLPe (stock #003800, Jackson Laboratory) that express the FLP recombinase under the direction of the ACTB promoter to ubiquitously delete the FRT-flanked sequence. Successively, *Satb1*$^{floxed/floxed}$ mice were crossed with either *CD11c*-Cre (Jackson Laboratory #008068) or *Vav1*-Cre (Jackson Laboratory #008610) mice.

Notch1-Rosa26 mice were kindly provided by Dr. B.Z. Stanger (University of Pennsylvania Perelman School of Medicine) and backcrossed for at least ten generations to a C57BL/6 background. These transgenic mice have a floxed version of Notch1 interrupted by a STOP codon at the permissive locus Rosa26. Notch1-Rosa26 mice were crossed with *Satb1*$^{floxed/floxed}$ *CD11c*-Cre-recombinase to obtain conditional triple transgenic mice that simultaneously overexpress Notch1 and ablate Satb1 expression in the CD11c compartment.

Galectin-1-deficient (*Lgals1*$^{-/-}$) mice were originally generated by F. Poirier (Jacques Monod Institut, Paris). OT-I and OT-II transgenic mice were purchased from Taconic. C57BL/6 and congenic CD45.1$^+$ mice (5–6 weeks old) were purchased from the Frederick Cancer Research Facility at the NCI.

All animals were maintained in pathogen-free barrier facilities. All experimental procedures were conducted in agreement with the institutional animal care and use committee of the Wistar Institute.

Parental ID8 cells were provided by K. Roby (Department of Anatomy and Cell Biology, University of Kansas Medical Center, Kansas City, KS) (Roby et al., 2000) and retrovirally transduced to express *Defb29* and *Vegf-a* (Conejo-Garcia et al., 2004). Flank tumors with ID8-*Defb29*-*Vegf-a* cells were admixed at a 10:1 ratio with BMDCs using factor-reduced Matrigel (BD Biosciences) and injected into the axillary flank. Tumor volume was calculated using the following equation: $(L \times W^2)/2$, where L is length and W is width. For retroviral transduction of Satb1, virus-containing media was produced transfecting the ecotropic Phoenix retroviral packaging cell line (Allele Biotech).

Mice bearing ID8-*Defb29*/*Vegf-a* tumors for 32–35 days were intraperitoneally (i.p.) injected with S100A9 (25 μg/mouse; Fitzgerald). After 36–48 hr, sorted tumor-associated DCs were analyzed for Satb1 expression as indicated.

Human Specimens

Advanced (stage III–IV) human ovarian carcinoma tissues were freshly procured under a protocol approved by the institutional review boards at Christiana Care Health System (#32214) and The Wistar Institute (#21212263). Informed consent was obtained from all subjects. Tumors were mechanically dissociated and directly analyzed or cryopreserved as viable single-cell suspensions for future analysis.

Generation of Bone Marrow Chimeras

Mononuclear BM cells collected from adult age-matched CD45.1 (congenic) wild-type or CD45.2 *Satb1*$^{-/-}$ donor mice ($1–2 \times 10^6$) were mixed in a 1:1 ratio and retro-orbitally injected into lethally irradiated (~950 rad) adult recipients. Mixed chimeras were analyzed after 7–8 weeks as indicated.

Antigen Presentation

For in vitro experiments, CD11c$^+$MHC II$^+$ sorted BMDCs (day 7) were incubated with 50 μg/ml full-length OVA (Sigma-Aldrich) for 3–15 hr, thoroughly washed, and co-cultured with Cell Trace Violet (Life Technologies)-stained OT-I or OT-II isolated T cells in a 1:10 ratio for 65–75 hr. T cell proliferation was analyzed by FACS on the basis of Cell Trace Violet and CD3$^+$CD8b$^+$ or CD3$^+$CD4$^+$, respectively. Division index was calculated by FlowJo.

Retroviral Transduction

Murine Satb1 cDNA (Source Bioscience) was subcloned into the retroviral expression vector pBMN-I-GFP (Addgene). BM cells were isolated from wild-type or *Lgals1*$^{-/-}$ mice and cultured as with GM-CSF for BMDC differentiation. At days 2 and 3 of culture, cells were washed and resuspended in Mock or *Satb1* pBMN virus-containing media supplemented with 8 mg/ml Polybreen (Millipore). Cells were then spin-infected at 2,500 rpm for 2 hr at 32°C, and the media was renewed 18 hr later. After 4 days of viral transduction, BMDCs were FACS sorted for GFP$^+$CD11c$^+$ and tested for different readouts as indicated.

In Vivo Delivery of PEI-siRNA Nanoparticles/Satb1 Silencing

Selective in vivo targeting of *Satb1* in tumor-associated DCs was previously described (Cubillos-Ruiz et al., 2009, 2012). In brief, murine on-Targeting (Ambion) or *Satb1* (Ambion or Integrated DNA Technologies) siRNA-polyethylenimine nanocomplexes were administered i.p. to mice bearing ID8-*Defb29*/*Vegf-a* tumors, using endotoxin-free "*in vivo*-Jet-PEI" FluoR at an N/P ratio of 6 following the recommendations of the manufacturer (Polyplus Transfection).

For survival, ELISPOTs, and phenotypic and antigen presentation experiments, ID8-*Defb29*/*Vegf-a*-challenged mice were i.p. treated with 50 μg siRNA-PEI nanocomplexes on days 8, 13, 18, 23, and 28 after tumor challenge. Survival was monitored periodically from this time point. For phenotypic experiments, total cells were obtained from red blood cell lysed peritoneal washes of siRNA-PEI-treated tumor-bearing mice 24 hr after the last treatment and analyzed by flow cytometry. Alternatively, total peritoneal cells were co-cultured for 48 hr, in coated and blocked ELISPOT plates with BMDCs (day 7) in a 10:1 ratio, which were previously pulsed (overnight) with gamma- and UV-irradiated ID8-*Defb29*/*Vegf-a* cells (10 DCs:1 tumor cell). Analysis for IFN-γ and Granzyme B spots was performed according to the manufacturer's protocol (eBioscience).

To test antigen presentation capabilities of tumor-associated-DCs in vivo, mice bearing ID8-*Defb29*/*Vegf-a* for 25–30 days were i.p. injected with 0.6 mg full-length OVA. After 3 hr, mice were either left untreated or injected i.p. with non-targeting or Satb1 siRNA-PEI nanocomplexes. Then, negatively isolated carboxyfluorescein succinimidyl ester (CFSE)-labeled CD3$^+$ OT-I splenocytes (2×10^6/mouse) were injected i.p. 18 hr after the siRNA treatment. 48 hr later, CD3$^+$CFSE$^+$OT-I$^+$ cells were harvested from peritoneal cavity and analyzed by FACS for proliferation.

ACCESSION NUMBERS

The accession number for the RNA-seq data reported in this paper is GEO: GSE76776. Additional details are available in Supplemental Experimental Procedures.

SUPPLEMENTAL INFORMATION

Supplemental Information includes Supplemental Experimental Procedures and one data file and can be found with this article online at http://dx.doi.org/10.1016/j.celrep.2016.01.056.

AUTHOR CONTRIBUTIONS

A.J.T. designed, performed, and analyzed most experiments. M.R.R. helped performing and designing flank tumor treatments and mice chimeras and in vivo DC mobilization. E.B. performed MLRs and phenotypic analysis of human samples. T.L.S. designed overexpression experiments and contributed to the generation of the Satb1 KO. M.J.A., N.S., and A.P.-P. performed and analyzed in vitro experiments and contributed to the design of in vivo experiments. J.M.N. did and analyzed in vitro experiments. M.E.B. and J.T. provided clinical specimens and expertise and helped write the manuscript. G.A.R. provided the galectin-1 KO and intellectual support and helped write the manuscript. J.W. and A.V.K. performed the bioinformatics analysis and provided intellectual support. J.R.C.-G. oversaw and designed the study and experiments, analyzed data, and co-wrote the manuscript.

ACKNOWLEDGMENTS

Support for Shared Resources was provided by Cancer Center Support Grant CA010815 to the Wistar Institute. We are grateful to the Flow Cytometry Facility at Wistar for outstanding technical insight, P. Jiang for the generation of Satb1-targeted mice, and Dr. B. Stanger (University of Pennsylvania) for generously providing the $Rosa^{Notch}$ mouse. This study was supported by grants R01CA157664, R01CA124515, R01CA178687, U54CA151662, and P30CA10815, the Jayne Koskinas & Ted Giovanis Breast Cancer Research Consortium at Wistar, and Ovarian Cancer Research Fund Program Project Development awards. M.J.A. and N.S. were supported by grant T32CA009171. A.P.-P. was supported by the Ann Schreiber Mentored Investigator Award (OCRF). A.J.T. was a nested Teal Scholar in Department of Defense grant OC100059.

Received: September 16, 2015
Revised: December 14, 2015
Accepted: January 14, 2016
Published: February 11, 2016

REFERENCES

Alvarez, J.D., Yasui, D.H., Niida, H., Joh, T., Loh, D.Y., and Kohwi-Shigematsu, T. (2000). The MAR-binding protein SATB1 orchestrates temporal and spatial expression of multiple genes during T-cell development. Genes Dev. *14*, 521–535.

Borghesi, L. (2014). Hematopoiesis in steady-state versus stress: self-renewal, lineage fate choice, and the conversion of danger signals into cytokine signals in hematopoietic stem cells. J. Immunol. *193*, 2053–2058.

Cai, S., Lee, C.C., and Kohwi-Shigematsu, T. (2006). SATB1 packages densely looped, transcriptionally active chromatin for coordinated expression of cytokine genes. Nat. Genet. *38*, 1278–1288.

Conejo-Garcia, J.R., Benencia, F., Courreges, M.C., Kang, E., Mohamed-Hadley, A., Buckanovich, R.J., Holtz, D.O., Jenkins, A., Na, H., Zhang, L., et al. (2004). Tumor-infiltrating dendritic cell precursors recruited by a beta-defensin contribute to vasculogenesis under the influence of Vegf-A. Nat. Med. *10*, 950–958.

Cubillos-Ruiz, J.R., Engle, X., Scarlett, U.K., Martinez, D., Barber, A., Elgueta, R., Wang, L., Nesbeth, Y., Durant, Y., Gewirtz, A.T., et al. (2009). Polyethylenimine-based siRNA nanocomplexes reprogram tumor-associated dendritic cells via TLR5 to elicit therapeutic antitumor immunity. J. Clin. Invest. *119*, 2231–2244.

Cubillos-Ruiz, J.R., Baird, J.R., Tesone, A.J., Rutkowski, M.R., Scarlett, U.K., Camposeco-Jacobs, A.L., Anadon-Arnillas, J., Harwood, N.M., Korc, M., Fiering, S.N., et al. (2012). Reprogramming tumor-associated dendritic cells in vivo using miRNA mimetics triggers protective immunity against ovarian cancer. Cancer Res. *72*, 1683–1693.

Cubillos-Ruiz, J.R., Silberman, P.C., Rutkowski, M.R., Chopra, S., Perales-Puchalt, A., Song, M., Zhang, S., Bettigole, S.E., Gupta, D., Holcomb, K., et al. (2015). ER Stress Sensor XBP1 Controls Anti-tumor Immunity by Disrupting Dendritic Cell Homeostasis. Cell *161*, 1527–1538.

Dalotto-Moreno, T., Croci, D.O., Cerliani, J.P., Martinez-Allo, V.C., Dergan-Dylon, S., Méndez-Huergo, S.P., Stupirski, J.C., Mazal, D., Osinaga, E., Toscano, M.A., et al. (2013). Targeting galectin-1 overcomes breast cancer-associated immunosuppression and prevents metastatic disease. Cancer Res. *73*, 1107–1117.

Helft, J., Böttcher, J., Chakravarty, P., Zelenay, S., Huotari, J., Schraml, B.U., Goubau, D., and Reis e Sousa, C. (2015). GM-CSF Mouse Bone Marrow Cultures Comprise a Heterogeneous Population of CD11c(+)MHCII(+) Macrophages and Dendritic Cells. Immunity *42*, 1197–1211.

Huarte, E., Cubillos-Ruiz, J.R., Nesbeth, Y.C., Scarlett, U.K., Martinez, D.G., Buckanovich, R.J., Benencia, F., Stan, R.V., Keler, T., Sarobe, P., et al. (2008). Depletion of dendritic cells delays ovarian cancer progression by boosting antitumor immunity. Cancer Res. *68*, 7684–7691.

Ilarregui, J.M., Croci, D.O., Bianco, G.A., Toscano, M.A., Salatino, M., Vermeulen, M.E., Geffner, J.R., and Rabinovich, G.A. (2009). Tolerogenic signals delivered by dendritic cells to T cells through a galectin-1-driven immunoregulatory circuit involving interleukin 27 and interleukin 10. Nat. Immunol. *10*, 981–991.

Joffre, O., Nolte, M.A., Spörri, R., and Reis e Sousa, C. (2009). Inflammatory signals in dendritic cell activation and the induction of adaptive immunity. Immunol. Rev. *227*, 234–247.

Lee, B.K., and Iyer, V.R. (2012). Genome-wide studies of CCCTC-binding factor (CTCF) and cohesin provide insight into chromatin structure and regulation. J. Biol. Chem. *287*, 30906–30913.

Lochamy, J., Rogers, E.M., and Boss, J.M. (2007). CREB and phospho-CREB interact with RFX5 and CIITA to regulate MHC class II genes. Mol. Immunol. *44*, 837–847.

Meredith, M.M., Liu, K., Darrasse-Jeze, G., Kamphorst, A.O., Schreiber, H.A., Guermonprez, P., Idoyaga, J., Cheong, C., Yao, K.H., Niec, R.E., and Nussenzweig, M.C. (2012). Expression of the zinc finger transcription factor zDC (Zbtb46, Btbd4) defines the classical dendritic cell lineage. J. Exp. Med. *209*, 1153–1165.

Murtaugh, L.C., Stanger, B.Z., Kwan, K.M., and Melton, D.A. (2003). Notch signaling controls multiple steps of pancreatic differentiation. Proc. Natl. Acad. Sci. USA *100*, 14920–14925.

Nakano, N., Nishiyama, C., Yagita, H., Koyanagi, A., Akiba, H., Chiba, S., Ogawa, H., and Okumura, K. (2009). Notch signaling confers antigen-presenting cell functions on mast cells. J. Allergy Clin. Immunol. *123*, 74–81.e1.

Nesbeth, Y., Scarlett, U., Cubillos-Ruiz, J., Martinez, D., Engle, X., Turk, M.J., and Conejo-Garcia, J.R. (2009). CCL5-mediated endogenous antitumor immunity elicited by adoptively transferred lymphocytes and dendritic cell depletion. Cancer Res. *69*, 6331–6338.

Notani, D., Gottimukkala, K.P., Jayani, R.S., Limaye, A.S., Damle, M.V., Mehta, S., Purbey, P.K., Joseph, J., and Galande, S. (2010). Global regulator SATB1 recruits beta-catenin and regulates T(H)2 differentiation in Wnt-dependent manner. PLoS Biol. *8*, e1000296.

Pavan Kumar, P., Purbey, P.K., Sinha, C.K., Notani, D., Limaye, A., Jayani, R.S., and Galande, S. (2006). Phosphorylation of SATB1, a global gene regulator, acts as a molecular switch regulating its transcriptional activity in vivo. Mol. Cell *22*, 231–243.

Roby, K.F., Taylor, C.C., Sweetwood, J.P., Cheng, Y., Pace, J.L., Tawfik, O., Persons, D.L., Smith, P.G., and Terranova, P.F. (2000). Development of a

syngeneic mouse model for events related to ovarian cancer. Carcinogenesis *21*, 585–591.

Rubinstein, N., Alvarez, M., Zwirner, N.W., Toscano, M.A., Ilarregui, J.M., Bravo, A., Mordoh, J., Fainboim, L., Podhajcer, O.L., and Rabinovich, G.A. (2004). Targeted inhibition of galectin-1 gene expression in tumor cells results in heightened T cell-mediated rejection; A potential mechanism of tumor-immune privilege. Cancer Cell *5*, 241–251.

Rutkowski, M.R., Stephen, T.L., Svoronos, N., Allegrezza, M.J., Tesone, A.J., Perales-Puchalt, A., Brencicova, E., Escovar-Fadul, X., Nguyen, J.M., Cadungog, M.G., et al. (2015). Microbially driven TLR5-dependent signaling governs distal malignant progression through tumor-promoting inflammation. Cancer Cell *27*, 27–40.

Satpathy, A.T., Kc, W., Albring, J.C., Edelson, B.T., Kretzer, N.M., Bhattacharya, D., Murphy, T.L., and Murphy, K.M. (2012). Zbtb46 expression distinguishes classical dendritic cells and their committed progenitors from other immune lineages. J. Exp. Med. *209*, 1135–1152.

Scarlett, U.K., Cubillos-Ruiz, J.R., Nesbeth, Y.C., Martinez, D.G., Engle, X., Gewirtz, A.T., Ahonen, C.L., and Conejo-Garcia, J.R. (2009). In situ stimulation of CD40 and Toll-like receptor 3 transforms ovarian cancer-infiltrating dendritic cells from immunosuppressive to immunostimulatory cells. Cancer Res. *69*, 7329–7337.

Scarlett, U.K., Rutkowski, M.R., Rauwerdink, A.M., Fields, J., Escovar-Fadul, X., Baird, J., Cubillos-Ruiz, J.R., Jacobs, A.C., Gonzalez, J.L., Weaver, J., et al. (2012). Ovarian cancer progression is controlled by phenotypic changes in dendritic cells. J. Exp. Med. *209*, 495–506.

Schraml, B.U., van Blijswijk, J., Zelenay, S., Whitney, P.G., Filby, A., Acton, S.E., Rogers, N.C., Moncaut, N., Carvajal, J.J., and Reis e Sousa, C. (2013). Genetic tracing via DNGR-1 expression history defines dendritic cells as a hematopoietic lineage. Cell *154*, 843–858.

Segura, E., and Amigorena, S. (2013). Inflammatory dendritic cells in mice and humans. Trends Immunol. *34*, 440–445.

Segura, E., Touzot, M., Bohineust, A., Cappuccio, A., Chiocchia, G., Hosmalin, A., Dalod, M., Soumelis, V., and Amigorena, S. (2013). Human inflammatory dendritic cells induce Th17 cell differentiation. Immunity *38*, 336–348.

Toscano, M.A., Bianco, G.A., Ilarregui, J.M., Croci, D.O., Correale, J., Hernandez, J.D., Zwirner, N.W., Poirier, F., Riley, E.M., Baum, L.G., and Rabinovich, G.A. (2007). Differential glycosylation of TH1, TH2 and TH-17 effector cells selectively regulates susceptibility to cell death. Nat. Immunol. *8*, 825–834.

Vega-Ramos, J., Roquilly, A., Zhan, Y., Young, L.J., Mintern, J.D., and Villadangos, J.A. (2014). Inflammation conditions mature dendritic cells to retain the capacity to present new antigens but with altered cytokine secretion function. J. Immunol. *193*, 3851–3859.

Yasui, D., Miyano, M., Cai, S., Varga-Weisz, P., and Kohwi-Shigematsu, T. (2002). SATB1 targets chromatin remodelling to regulate genes over long distances. Nature *419*, 641–645.

Zhou, J., Cheng, P., Youn, J.I., Cotter, M.J., and Gabrilovich, D.I. (2009). Notch and wingless signaling cooperate in regulation of dendritic cell differentiation. Immunity *30*, 845–859.